Applied Thermal Engineering 88 (2015) 369–375

Contents lists available at ScienceDirect

Applied Thermal Engineering

journal homepage: www.elsevier.com/locate/apthermeng

Numerical analysis of a novel ground heat exchanger coupled with phase change materials

Michele Bottarelli [a,*], Marco Bortoloni [b], Yuehong Su [c], Charles Yousif [d], Ahmet Alper Aydın [e], Aleksandar Georgiev [f]

[a] Department of Architecture, University of Ferrara, Via Quartieri 8, Ferrara 44121, Italy
[b] Department of Engineering, University of Ferrara, Via Saragat 1, Ferrara 44122, Italy
[c] Department of Architecture and Built Environment, University of Nottingham, University Park NG7 2RD, UK
[d] Institute for Sustainable Energy, University of Malta, Barrakki Street, Marsaxlokk MXK 1531, Malta
[e] Chemical Engineering Department, Faculty of Chemical and Metallurgical Engineering, Istanbul Technical University, 34469 Maslak, Istanbul, Turkey
[f] Department of Mechanics, Technical University of Sofia, 25 Tsanko Diustabanov St., Plovdiv 4000, Bulgaria

HIGHLIGHTS

- Coupling of a flat-panel ground source heat exchanger (GHE) with PCMs.
- The mixture of soil and PCMs is assumed as a backfill material for the GHE.
- Numerical simulation of heat transfer in soil with realistic boundary conditions.
- PCMs allow better working fluid temperatures mitigating the soil's thermal depletion.
- Potential increase in the COP of a ground coupled heat pump.

ARTICLE INFO

Article history:
Received 14 June 2014
Received in revised form
29 September 2014
Accepted 7 October 2014
Available online 15 October 2014

Keywords:
Ground-coupled heat pump
Ground heat exchanger
Flat-panel
Phase change materials
Numerical model
Underground thermal energy storage

ABSTRACT

Thermal energy storage with phase change materials (PCMs) is a functional strategy to minimize the sizing of air conditioning systems and reduce their primary energy consumption. This approach is well known in ground-coupled heat pump applications (GCHP), especially with use of borehole ground heat exchangers (GHEs). However, this is seldom investigated for coupling with shallow horizontal GHEs that are usually considered to be less effective for GCHP applications, due to faster depletion of the stored thermal energy as a result of the seasonal energy balance.

In order to make shallow GHEs more effective, mixing PCMs directly with backfill material for a flat-panel type GHE is presented in this study. The application has been evaluated through numerical modelling to solve transient heat transfer using effective heat capacity method. Yearly performance has been simulated by taking into account the estimated energy requirement for an assumed residential building located in Northern Italy. According to hourly time series boundary conditions and annual performance, the simulation results show that employment of PCMs is able to smooth the thermal wave in the ground, improve the coefficient of performance of the heat pump (COP) and if suitably sized, prevent thermal depletion in winter by charging the PCMs naturally in summer with a shallow GHE.

1. Introduction

Ground-coupled heat pumps (GCHPs) have been regarded as a sustainable energy technology for space heating and cooling in commercial, industrial and residential buildings, as well as a profitable solution when correctly designed. Coupling a heat pump with the ground is obtained by means of ground heat exchangers (GHEs), which can be installed vertically or horizontally. In the horizontal installation, the heat exchangers are placed in shallow diggings a few metres deep in soil, as opposed to the vertical solution where the heat exchangers are installed in boreholes drilled down up to a hundred metres deep. Owing to their different depths of installation, the vertical solution exploits a real geothermal

* Corresponding author. Tel.: +39 0532 293653.
E-mail addresses: michele.bottarelli@unife.it (M. Bottarelli), marco.bortoloni@unife.it (M. Bortoloni), yuehong.su@nottingham.ac.uk (Y. Su), charles.yousif@um.edu.mt (C. Yousif), aydinal@itu.edu.tr (A.A. Aydın), ageorgiev@gmx.de (A. Georgiev).

http://dx.doi.org/10.1016/j.applthermaleng.2014.10.016
1359-4311/

source, while for the horizontal one, the ground source may mainly serve as a solar energy buffer. However, the weakest link in a GCHP system is the GHE, because the heat transfer in the ground is mainly conductive and its thermal diffusivity is low. This means that the ground thermal response is much slower than the heat pump requirement, resulting in thermal waves being transmitted into the ground through the GHEs by means of a circulation loop. This may cause lower coefficient of performance of a GCHP, because the heat pump has to lower its evaporation temperature in winter or increase its condensation temperature in summer to obtain the required heat flux. But, the heat pump usually operates in an alternate on/off mode, so it would be interesting to apply ground thermal storage to suppress the thermal wave by use of the off-time thermal buffer to maintain on-time heat flux requirement.

Employing Phase Change Materials (PCMs) is an effective measure to store thermal energy [1,2] and it may also be considered as an effective method to smooth the thermal wave generated from operation of a GCHP [3,4]. In this study, we propose to mix the PCMs directly with backfill material in a trench containing a flat-panel GHE. The backfill material could be also contained in a shell close to the GHE. There is little research reported in literature about this idea [5–8], and the performance has not yet been investigated for shallow GHEs. Use of the PCMs incorporated with GHEs may be able to meet some instantaneous high heat flux demand by a GCHP, thus reducing the sudden heating or cooling thermal wave upon the ground. Therefore, the peak operation temperature in the heating/cooling mode of a GCHP could be raised/lowered for a given size of GHE. In other words, the GHE size could be reduced for a given peak operation temperature. Moreover, the depletion of the latent heat due to the PCMs solidification/melting could be recharged during the summer/winter season, which therefore achieves the seasonal ground thermal storage.

2. Methodology and numerical simulation

The coupling between the GHE and PCMs is here assumed to occur by mixing water and micro-encapsulated paraffin with the soil, and use the mixture as a backfill material for the trench containing a flat-panel GHE. Due to different solidification/melting temperatures, water in the mixture is devoted to prevent depletion of heat in the low temperature situation (heating season in winter), whereas micro-encapsulated paraffin is required for the high temperature situation (cooling season in summer). The numerical approach was simplified by considering the heat conduction problem of an equivalent solid to the supposed mixture, and to solve it numerically by means of a commercial software (COMSOL Multiphysics, V4.4).

The model is implemented in a 2D domain with time-varying boundary conditions to study the temperature distribution in the ground and at the surface of GHE, by solving the equation:

$$\rho_{eq} c_{eq} \frac{\partial T}{\partial t} = \nabla \cdot (\lambda_{eq} \nabla T) \tag{1}$$

where ρ_{eq}, c_{eq} and λ_{eq} are the equivalent density, specific heat and heat conductivity of the mixture, which can be calculated as the mass weighted average properties of the mixture at the given temperature. In addition, the latent heat of fusion is considered in c_{eq}. To represent those thermo-physical properties during the phase change, some specific relationship are implemented as an evolution of what is reported in Ref. [9]. In the reported approach, the PCM problem was numerically treated as a simple porous media, which is composed of the two phases of the same material (e.g., solid ice and liquid water). The specific heat capacity c was defined to consider the latent heat of fusion h^{SL} by means of a normalized Dirac's pulse $D(T)$, expressed in K^{-1}. Moreover, the phase change between the liquid phase (L) and the solid one (S) are expressed in Ref. [9] as a function of a dimensionless variable $H(T)$ which is the volumetric fraction of the liquid phase in a PCM, ranging between 0 and 1 with respect to the temperature changing around the melting point (T_m). These functions were introduced to moderate the switching between solid ($H(T_m - \Delta T) = 0$) and liquid phases ($H(T_m + \Delta T) = 1$).

In the present study, because of working with two different PCMs ($n = 2$) and considering only heat conduction, we simplified the porous media heat transfer as a heat conduction problem of an equivalent solid domain. Here, the solid matter is considered as a mixture between soil and the two PCMs, in accordance with the respective mass ratio r_i supposed between each PCM and the soil (G). As a consequence and in variation of a previous work [9], two different functions $H_i(T)$ were assumed as mass ratio of each specific PCM considered, and similarly two different functions $D_i(T)$ were used. The $H_i(T)$ and $D_i(T)$ functions for water and micro-encapsulated paraffin are given in Fig. 1, with evidence of their melting points.

Finally, the equivalent overall density, thermal conductivity and specific heat of the mixed backfill material were obtained as a mass weighted average of the total liquid and solid mass at a given temperature, as reported in the following equations with evidence of the variables:

$$\rho_{eq} = \left(1 - \sum_{i=1}^{n} r_i\right) \cdot \rho_G + \sum_{i=1}^{n} r_i \cdot (1 - H_i(T)) \cdot \rho_i^S + \sum_{i=1}^{n} r_i \cdot \rho_i^L \cdot H_i(T) \tag{2}$$

$$\lambda_{eq} = \left(1 - \sum_{i=1}^{n} r_i\right) \cdot \lambda_G + \sum_{i=1}^{n} r_i \cdot (1 - H_i(T)) \cdot \lambda_i^S + \sum_{i=1}^{n} r_i \cdot H_i(T) \cdot \lambda_i^L \tag{3}$$

$$c_{eq} = \left(1 - \sum_{i=1}^{n} r_i\right) \cdot c_G + \sum_{i=1}^{n} r_i \cdot (1 - H_i(T)) \cdot \left(c_i^S + h_i^{SL} \cdot D_i(T)\right) + \sum_{i=1}^{n} r_i \cdot H_i(T) \cdot \left(c_i^L + h_i^{SL} \cdot D_i(T)\right) \tag{4}$$

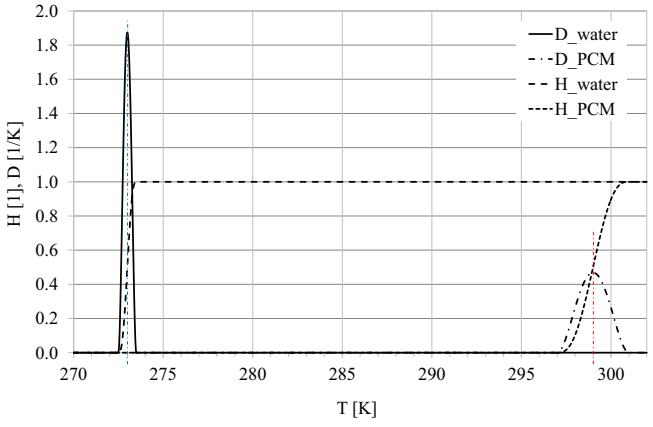

Fig. 1. D & H functions indicating the phase change of water and paraffin.

2.1. Model domain

The model domain considers a cross section which comprises a PCM layer and a wide surrounding soil part. The PCM layer as described above is a mix of micro-encapsulated paraffin, water and soil with specified mass ratios.

A symmetric approach was considered so that half of the domain could be analysed in order to reduce the finite elements calculation. The GHE is assumed to be a flat-panel that shows high heat transfer capacity, as reported in Ref. [10]. It is easy to reproduce this in a 2D approach, hence the flat-panel is introduced as a boundary condition of the numerical domain.

As presented in Fig. 2, the size of the domain is 10 m wide and 15 m deep. The GHE is 1 m high and it is laid between 1.3 and 2.3 m deep. The PCM layer is placed between 0.8 and 2.5 m deep; its thickness is assumed to be equal to 0.30 m and the resulting volume of PCM layer for each metre of flat-panel length is 0.51 m^3. The dimensions were chosen to be similar to those in a field trial, which is under testing at the Department of Architecture at the University of Ferrara, Italy, to compare modelling to experimental results in the near future.

To minimize the numerical errors and to expedite the computation, the size of the finite elements was chosen to be fine for the area close to the GHE and coarse for the area far from it. The full mesh is shown in Fig. 3 and it is limited to 23,000 elements to reduce the computational time. Almost 18,000 elements are reserved for the PCM layer, so the resulting grid size is between 0.16 cm^2 for fine grids and 0.16 m^2 for coarse grids.

To check the mesh independence of the solutions, the same problem in steady state case was solved with a mesh increased to more than 50,000 elements, and it was found there is a negligible change in the numerical solution.

2.2. Initial and boundary conditions

The initial condition of the unsteady state thermal analysis was obtained by executing the model in absence of the GHE activity and starting with an initial uniform domain temperature of 15 °C. This temperature was taken as yearly average of the time series of the air temperature that would be also assumed for the energy requirement analysis of the GHE. After simulation for the third year, no evidence of thermal drift was present and thus this solution was assumed as initial condition.

Boundary conditions of the 1st and 2nd kind were used at the outer domain boundaries as thermal conditions for solving the numerical problem of heat transfer in solid. At the bottom of the domain, a constant temperature of 15 °C was assumed, representing undisturbed conditions. The right side of the domain was assumed adiabatic, and similarly the left side with exception of the GHE wall, where an hourly time varying heat flux was applied to represent the energy requirement in heating and cooling modes of a GCHP system. Finally, a further hourly time varying heat flux was imposed at the ground surface to represent the shallow energy balance. Both the heat flux boundary conditions had been calculated from a sinusoidal time series assumed for the air temperature, as specified below.

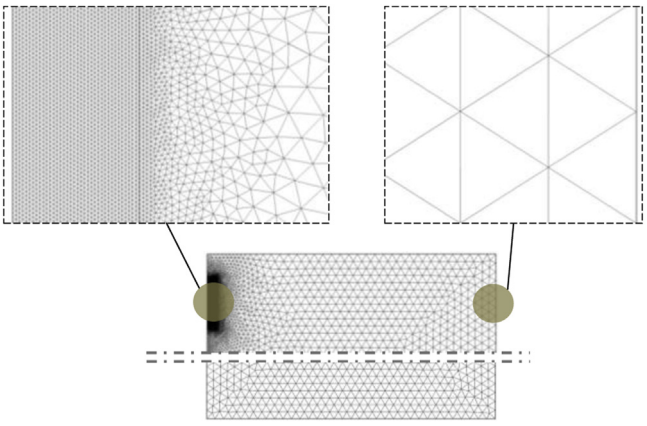

Fig. 3. Mesh details.

2.2.1. GCHP heating and cooling loads

To define the hourly heating and cooling loads, we adopted the simplified methodology as reported in previous study [10,11], i.e., to consider the maximum heat transfer through the shell of a building. The building was considered as a homogenous lumped system, whose internal energy variation occurs owing to the heat transfer through its shell in response to the outdoor air temperature time series. The GCHP operation hours are selected to represent typical working conditions at the residential scale in a mild climate: 5–9 am and 4–11 pm from Monday to Friday, and from 7 am to 12 pm on weekends. The system is operated in heating mode from October 13th to May 16th, and in cooling mode for the remaining days.

Neglecting indoor passive contributions, when the air conditioning plant is supposedly turned off, the variation in time series of the indoor air temperature can be estimated in accordance with the

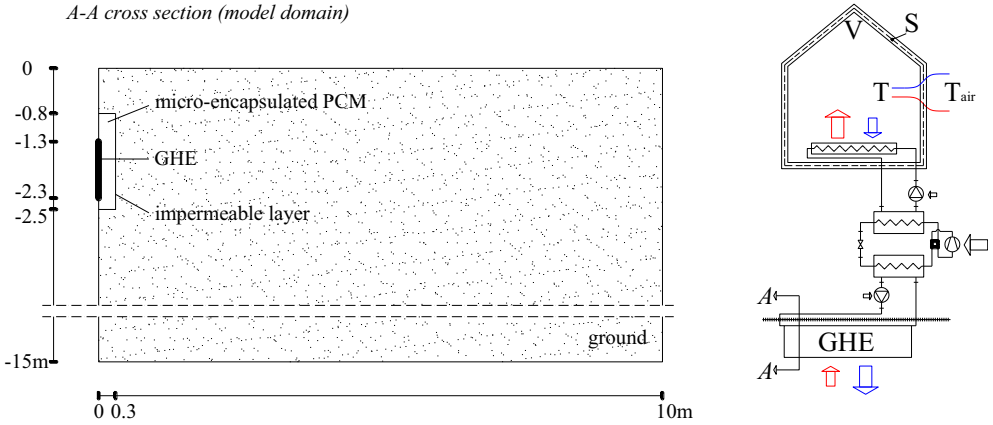

Fig. 2. Sketch of the one-half symmetric model domain of a GHE and its coupling with a heat pump.

energy balance, which is influenced on one hand by the heat transfer through the envelope, and on the other, by the building's total internal energy variation. In turn, the latter is basically represented by the mass of roof, walls and floors. For simplicity, we assumed the building as a lumped system with a very small *Biot* number ($Bi \ll 1$), to give a uniform temperature in the whole building envelope. Thus, given the building global equivalent thermal transmittance (U), heat transfer surface area of the envelope (S), global building volume (V), average density (ρ_b) and specific heat (c_b, evaluated as weighted averages of the densities and specific heats of the individual building elements), and ratio (r_b) between fabric over global building volume, the energy balance for the off-period of heat pump can be written at each time step as:

$$r_b V \cdot \rho_b c_b \cdot dT = -U \cdot S \cdot \left(T(t) - T^{air}(t)\right) \cdot dt \quad (5)$$

where T and T^{air} are the indoor and outdoor air temperatures at time step t. Assuming the outdoor air temperature to be independent from heat transfer, Equation (5) can be easily integrated as:

$$T(t) = T^{air}(t) + \left(T_{off} - T^{air}(t)\right) \cdot e^{-\frac{US \cdot \left(t - t_{off}\right)}{r_b V \cdot \rho_b c_b}} \quad (6)$$

where T_{off} is the indoor air temperatures at time t_{off}, when the heat pump is switched off, and S/V is the shape ratio of the building. Equation (6) gives the indoor air temperature change during the off-period of heat pump.

When the plant is switched on at time t_{on}, after an off-period, a constant target value $T^{h/c}$ can be assumed for the indoor temperature (20 °C in heating, 25 °C in cooling). Then, the energy demand for each cubic metre of building over a time step Δt can be estimated as the sum of the energy needed to reach the target temperature starting from a cooler/warmer temperature occurred due to the off-period $T(t_{on})$, and the heat transfer due to the difference between the indoor air temperature and the outdoor temperature $T^{air}(t_{on})$:

$$q(t_{on}) = U \cdot \frac{S}{V} \cdot \left(T^{h/c} - T^{air}(t_{on})\right) \cdot \Delta t + r_b \cdot \rho_b c_b \cdot \left(T^{h/c} - T(t_{on})\right) \quad (7)$$

Because of the assumed maximum heating/cooling power of 30 W/m^3 (P_{max}) given by the heat pump, the indoor target temperature could not be achieved for the first few time step Δt. So, for this situation, instead of a constant value, the $T^{h/c}$ temperature is obtained using Equation (7), but setting $q(t_{on}) = P_{max} \cdot \Delta t$.

For simplicity, we assumed that the above heating/cooling energy is the same as that delivered by the closed GHE loop; it means that the heat pump compressor is assumed to work only to raise the closed loop to the required temperature. Moreover, we assumed that each metre of GHE flat-panel provides energy for 3.6 m^3 of building, according to the assumed GHE maximum heat flux of 110 W per square metres of flat-panel.

In Table 1 the building parameters are described to estimate the energy requirement as previously presented. Furthermore, Figs. 4 and 5 show the resulting time series at yearly and weekly scales, the last one to appreciate the hourly behaviour. The supposed simplification affects in particular the transition period between the winter and summer, where the off mode of heat pump impacts largely over the indoor temperature. As a consequence, the plant works at the maximum power for a long time and causes a larger energy requirement than that required in continuous mode operation during the weekend. Even if this behaviour is expensive and not suitable, it is here accepted because it is not the focus of the present analysis and represents only an energy demand time series in order to study the dynamic behaviour of the GHE incorporated with PCMs.

Table 1
Energy requirement data.

Description	Symbol	Value	Unit
Building envelope shape ratio	S/V	0.5	m^{-1}
Equivalent thermal transmittance	U	0.5	W/m^2 K
Ratio of fabric over building volume	r_b	0.1	–
Average wall density	ρ_b	900	kg/m^3
Average wall specific heat	c_b	1200	J/kg K
Indoor target temperature in winter	T^h	20	°C
Indoor target temperature in summer	T^c	25	°C
Heating season	–	215	Days
Cooling season	–	150	Days
Operating hours in heating mode	–	2750	Hours
Operating hours in cooling mode	–	1474	Hours
Maximum daily air temperature in winter	T_w^{max}	4	°C
Minimum daily air temperature in winter	T_w^{min}	−2	°C
Maximum daily air temperature in summer	T_s^{max}	39	°C
Minimum daily air temperature in summer	T_s^{min}	26	°C
Day of year of the minimum air temperature	–	30	DOY
Resulting heating degree-days	–	2534	Day K
Resulting cooling degree-days	–	789	Day K
Soil–air coefficient	R	0.6	–
Overall energy requirement in heating (semi-GHE)	–	51.3	kWh/m^2
Overall energy requirement in cooling (semi-GHE)	–	16.0	kWh/m^2
Maximum daily energy requirement in heating (semi-GHE)	–	0.398	kWh/day
Maximum daily energy requirement in cooling (semi-GHE)	–	0.278	kWh/day
Daily average energy requirement in heating (semi-GHE)	–	0.245	kWh/day
Daily average energy requirement in cooling (semi-GHE)	–	0.113	kWh/day

2.2.2. Ground surface heat flux

Since there were not enough data available to provide a meaningful estimation of the ground surface energy balance and then to introduce a 3rd kind boundary condition, we obtained the net soil surface heat flux as an indirect solution from a preparatory run of the model without any GHE activity. In this run, the sinusoidal time series of the air temperature adopted for the previous analysis is imposed at the soil surface, by means of reducing coefficient of the oscillatory amplitude to be 0.6. This value was chosen in accordance to the temperatures monitored at the soil surface in a trial field

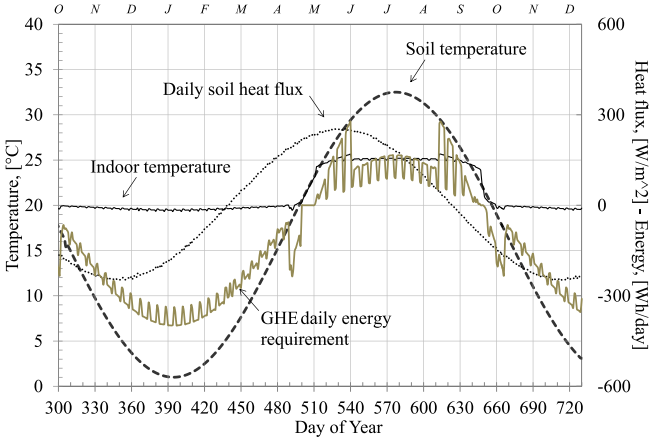

Fig. 4. Daily time series of the simplified boundary conditions.

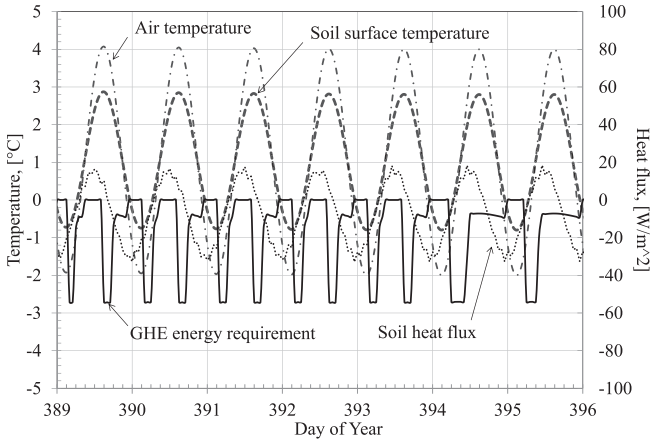

Fig. 5. Hourly time series of the simplified boundary conditions as implemented in the model.

operating at the Department of Architecture of Ferrara University, Italy.

The preparatory model was run for the period of three years, and the resulting heat flux density at the soil surface was obtained from the model. The building data and the energy requirements in heating and cooling seasons are summarized in Table 1; the daily heat flux time series at the GHE is presented in Fig. 4, and an hourly detail is depicted in Fig. 5, where the time at the axis is selected to have a full winter and summer operating span.

For the selected air temperature time series, the resulting values are included in the interval ±60 W/m^2, and the corresponding cumulative energy balance oscillates in the range ±15 kWh/m^2 per year. Similar data are reported in Refs. [12,13], where it is specified that the surface soil heat flux typically represents 1–10% of the net solar radiation.

2.3. Material properties

The materials making up the domain are soil, water and a specific mixture of paraffin, whose melting point is around 26 °C. The soil filling all around the domain is considered dry and unchangeable with the exception of the layer reserved for the GHE backfill material. Inside this layer, the soil is assumed to be saturated with water and mixed with micro-encapsulated paraffin, according to its mass ratio (70%) and those of water (20%) and paraffin (10%). In the absence of the PCMs, the soil filling the trench is only characterized by the properties of the rock matter in accordance to the previous mass ratio (70%), and the resulting porosity (30%). The micro-encapsulated solution is here considered as a material that causes no chemical or physical harm to the environment. The generalized thermal properties of paraffin are defined according to the thermal data of fatty acid ester based PCMs in Refs. [14,15] and for water and ice, they are taken from data in literature, e.g. in Ref. [16].

To avoid introducing the moving mesh method which ensures mass conservation when density variations occur in phase change, we assumed that the density of each PCM does not change between the solid and liquid phases, given their average value in the analysis. This inaccuracy should not affect much, because the thermal problem is focused on the high latent heat. Moreover, the mass of the mixed PCMs is very low in comparison with the soil.

According to the previous remarks, the values of mass ratio (r), latent heat (h^{SL}), melting point (T_m), density (ρ), specific heat (c) and heat conductivity (λ) for the materials are summarised in Table 2.

Table 2
Material properties.

	h^{SL} (kJ/kg)	T_m (K)	ρ (kg/m^3)	c (kJ/kg K)	λ (W/m K)	r (%)	Note
Soil^{domain}	–	–	1800	1200	1.00	–	Soil outside the trench
Soil^{bulk}	–	–	1600	1000	1.20	–	Soil without PCMs
Soil^{rock}	–	–	2286	1428	1.71	70	Rock constituent
Paraffin^{solid}	214	299 ± 2.0	790	2200	0.21	(20)	
Paraffin^{liquid}	214	299 ± 2.0	790	2200	0.21	(20)	
Water	334	273 ± 0.5	959	4230	0.57	(10)	
Ice	334	273 ± 0.5	959	2040	1.88	(10)	

3. Results and discussions

To compare the impact of the PCMs on the ground thermal field and then on the temperature of the GHE working fluid, the cases with and without PCMs have been solved for a simulation period of two years. The second year has been executed to check the seasonal periodic oscillation and to evaluate the thermal drift operated by the GHE. Indeed, the heat flux applied at the soil surface does not consider the thermal impact of the GHE operation, because it has been inversely calculated from a model with a fixed temperature over the surface, which was not modified by this action. Thus, it should be expected that the yearly final temperature of the thermal field could be different from the initial one. Nevertheless, if the same difference of temperature appeared also in the second simulation year, it can be concluded that the model was in a stationary trend. It has been checked that the ground temperature at the position 1.8 m deep and 10 m away from the GHE changes by 0.3 °C both at the end of the first year and at the end of the second one, solely caused by the operation of the GHE. With this approximation, the simulation results are discussed as follows.

Figs. 6 and 7 show the simulated yearly time series of the temperatures for the selected grid points in the domain and for the two cases with and without phase change materials, respectively. The *G_GHE* and *PCM_GHE* curves are the average temperatures along the GHE wall for the case without phase change materials (case *G*) and with it (case *PCM*). The other temperatures are for those points at the same depth as the middle of the GHE, with the distance of 0.1, 0.2, 0.5 and 10.0 m away from the GHE, respectively. The first two points are inside the trench, whereas the two other ones are outside. In comparison with the presence of PCM, the case

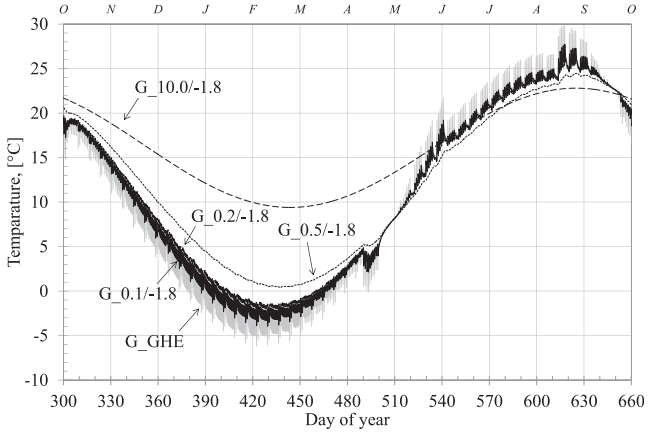

Fig. 6. Simulated time series temperatures over one year for the case G without phase change materials.

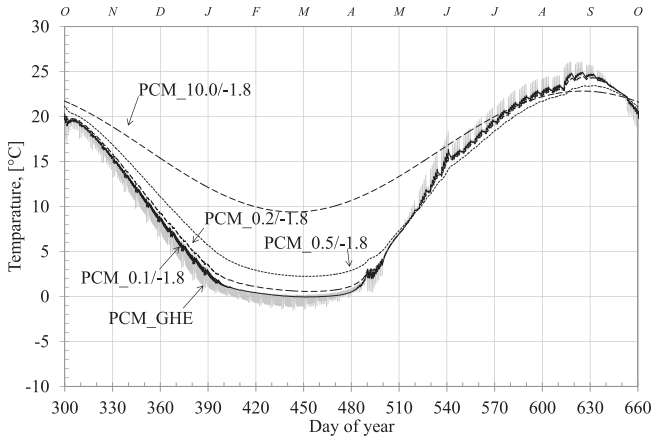

Fig. 7. Simulated time series temperatures over one year for the case with PCMs (phase change materials).

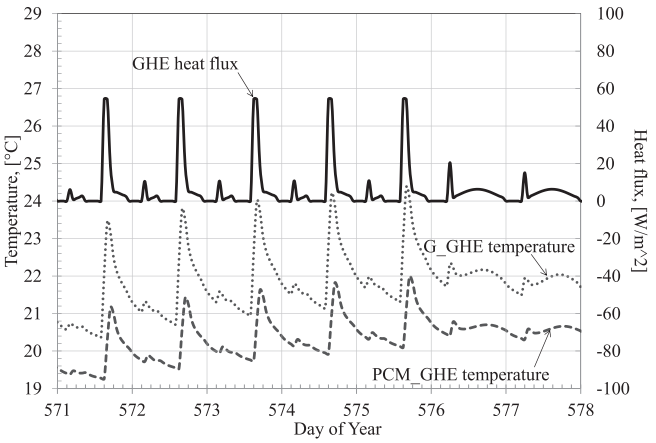

Fig. 9. Simulated time series temperatures for one week in summertime.

G without PCM shows lower temperatures in winter that drop down to −6 °C, whereas the case with PCM reaches −1 °C, due to freezing. Interesting is also the behaviour of the oscillations; for the case G without PCM, the working fluid changes its daily temperature by several degrees between the minimum and maximum values, whereas for the case with PCM, the oscillation is limited to 1–2 °C, with evidence of a smoothing action performed by the change of phase. Moreover, the point 0.5 m away from the GHE still shows oscillations in the case G without PCM, unlike the same point in the case with PCM. Furthermore, the maximum temperature of the case G without PCM is around 30 °C, unlike that of the case with PCM, which does not go above 26 °C. For both cases, when the plant is turned off at end of summer, the temperatures quickly reach that of the undisturbed condition (10.0 m away & 1.8 m deep). Finally, there are no differences between the two cases for the point farther away from the GHE, indicating the absence of different behaviour so far from the GHE. In summer, a less frequent switch between the on/off GHE modes is evident.

As shown in Figs. 8 and 9, the simulation results for a week are chosen to depict the diurnal time series of the temperatures along the GHE wall for both cases, together with the heat flux. A different behaviour is here detailed for one week both in winter and in summer, with evidence of different temperature variations. The PCM case shows average temperatures at the GHE wall up to 5 K higher than the case without PCM during the week (422 and 423 DOY), which needs a very different work for the heat pump and also could allow use of water as the working fluid without adding glycol.

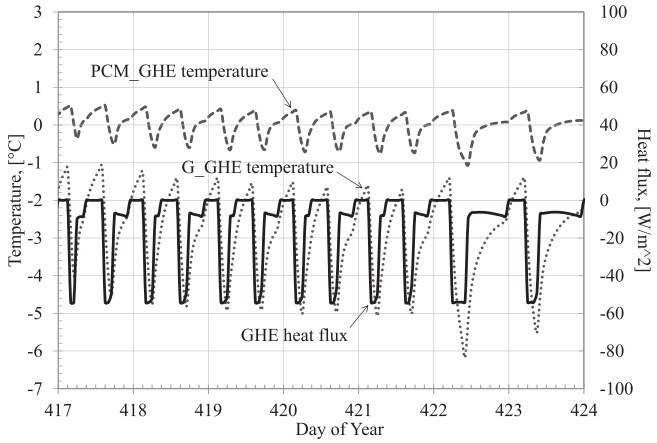

Fig. 8. Simulated time series temperatures for one week in wintertime.

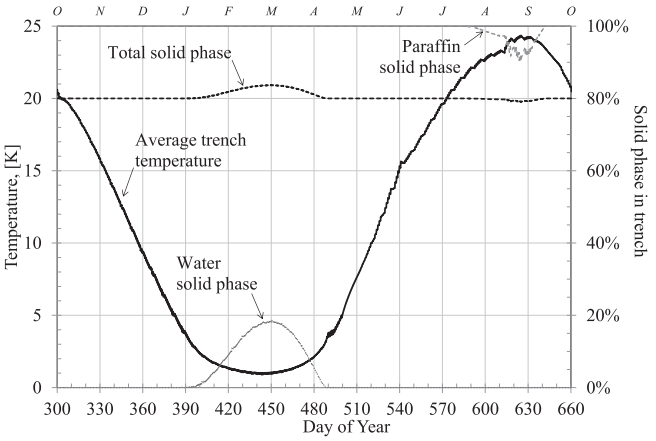

Fig. 10. Simulated time series of the solid phase fraction inside the trench.

In Fig. 10, the overall solid phase time series for the trench is reported in terms of mass ratio, together with the average temperature of the trench, and the solid phase fraction for both water and paraffin are detailed. The freezing of the water starts at 390 DOY and ends at 490 DOY. Even if the effect on the temperature is clear, only a maximum of 20% of water saturating the trench

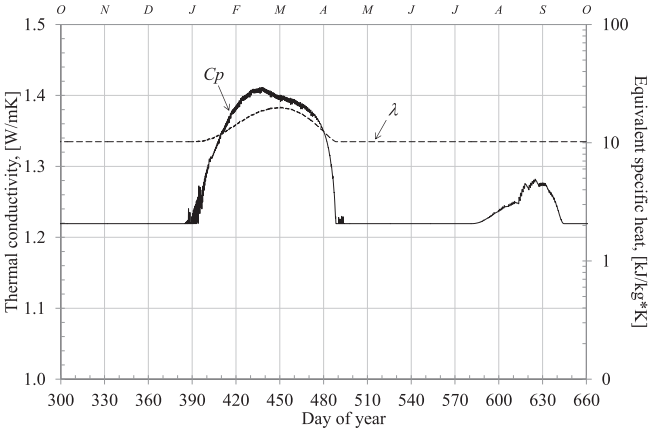

Fig. 11. Simulated time series of the equivalent specific heat and thermal conductivity.

freezes. It implies that there is still an energy surplus that could be potentially available by the phase change of the residual liquid water, and thus the exploitation would have been prolonged even with higher power at the GHE. In summer, the melting of the paraffin starts around 580 DOY and ends at 640 DOY; the maximum melting reaches 10% of the paraffin mass mixed with the soil. This low effect is related to the melting point selected for the PCM, in accordance with the natural temperature of the soil and the heat flux at the GHE. Probably, a lower melting point would have been more suitable for the present application.

Finally, Fig. 11 shows how the equivalent specific heat and the thermal conductivity of the mixed soil change inside the trench; the values are the average of the overall material inside the trench. In winter, both parameters change, whereas in summer the heat conductivity is stable because the value does not change for the paraffin from solid to liquid phase. According to the above-mentioned energy surplus potentially available by the phase change of the residual liquid water, the icing does not represent a limit in the heat transfer of the system, because of the higher heat conductivity of the ice in comparison with the liquid water, as well emphasized in Ref. [17].

4. Conclusions

The coupling between phase change materials (PCMs) and ground heat exchangers (GHEs) has been proposed to analyse the potential energy saving benefits in an unsteady heat transfer problem of a ground-coupled heat pump (GCHP), for space heating and cooling. Micro-encapsulated paraffin and water are assumed as PCMs to be mixed directly with backfill material surrounding the GHEs. The application is evaluated through numerical modelling to solve the heat transfer of a simply conduction problem in an equivalent solid, whose thermal properties are combined to express the phase change of the two PCMs considered.

In a 2D domain, a flat-panel GHE has been assumed to be operating in accordance with the hourly heating and cooling loads of a simplified model building, supplied with a GCHP. The hourly time series air temperature has been obtained according to the on/off time scheduling of the heat pump, in order to approach a realistic case.

In comparison with the case without PCMs, the surface temperatures of the GHE coupled with PCMs could be higher in winter and lower in summer by several degrees. This indicates the potential increase in the coefficient of performance of the heat pump. Furthermore, an interesting effect of smoothing of the thermal wave generated by the heat pump is clear.

The presented design may indicate a new opportunity for shallow horizontal GHEs. Unlike the vertical and deep borehole GHEs, it is normally believed that it is unsuitable to attempt the underground thermal energy storage (UTES) for shallow GHEs, because its surrounding soil is more apt to the effect of the weather and seasonal change. Coupling with PCMs can mitigate the depletion of stored thermal energy and thus enhance the UTES opportunity for shallow GHEs.

Acknowledgements

The authors thank the University of Ferrara, Italy (no. 19488/2011), for funding the start-up of the present workgroup by means of International Grants 2011.

References

[1] G.S.H. Lock, Latent Heat Transfer – an Introduction to Fundamentals, Oxford University Press, London, 1996.
[2] M.M. Farida, A.M. Khudhaira, S.A.K. Razackb, S. Al-Hallajb, A review on phase change energy storage: materials and applications, Energy Convers. Manag. 45 (9–10) (2004) 1597–1615.
[3] E. Lohrenx, S. Almeida, Ground-coupled heat pump and energy storage, ASHARAE J. 55 (4) (2013) 14–22.
[4] Y. Rabin, E. Korin, Incorporation of phase-change materials into a ground thermal energy storage system: theoretical study, J. Energy Resour. Technol. Trans. ASME 118 (3) (1996) 237–241.
[5] L. Haiyan, Z. Neng, Analysis of phase change materials (PCMs) used for borehole fill materials, in: Geothermal Resources Council Annual Meeting 2009, vol. 33, 2009, pp. 83–88.
[6] M. Bottarelli, M. Bortoloni, A. Georgiev, A.A. Aydin, Y. Su, C. Yousif, Ground-source heat pumps: benefits of using phase change materials, in: 2nd Int. Conf. of Sustainable Energy Storage in Buildings, Trinity College Dublin, 2013.
[7] M. Bottarelli, A. Georgiev, A.A. Aydin, Y. Su, C. Yousif, Ground-source heat pumps using phase change materials, in: European Geothermal Congress, Pisa, 2013.
[8] H. Lei, C. Dai, Comparative experiment of different backfill grouts for concentric ground heat exchangers, Trans. Geotherm. Resour. Counc. 37 (part 2) (2013) 597–600.
[9] COMSOL Multiphysics Model Library, COMSOL Inc., 2012.
[10] M. Bottarelli, V. Di Federico, Numerical comparison between two advanced HGHEs, Int. J. Low-Carbon Technol. 7 (2012) 75–81.
[11] M. Bottarelli, L. Gabrielli, Payback period for a ground source heat pump system, Int. J. Heat Technol. 29 (2011) 145–150.
[12] T.J. Sauer, R. Horton, Soil heat flux, pp. 131–154, in: J.L. Hatfield, J.M. Baker (Eds.), Micrometeorology in Agricultural Systems, Agronomy, Madison, WI, 2005, p. 584.
[13] D. Hillel, Introduction to Soil Physics, Academic Press, 1982.
[14] A.A. Aydin, High-chain fatty acid esters of 1-octadecanol as novel organic phase change materials and mathematical correlations for estimating the thermal properties of higher fatty acid esters' homologous series, Sol. Energy Mater. Sol. Cells 113 (2013) 44–51.
[15] A.A. Aydin, Fatty acid ester-based commercial products as potential new phase change materials (PCMs) for thermal energy storage, Sol. Energy Mater. Sol. Cells 108 (2013) 98–104.
[16] Y.A. Çengel, Heat and Mass Transfer: a Practical Approach, third ed., McGraw-Hill Education, 2007.
[17] G. Gan, Dynamic thermal modelling of horizontal ground-source heat pumps, Int. J. Low-Carbon Technol. 8 (2013) 95–105.